ORNL/TM-10854

OAK RIDGE NATIONAL LABORATORY

MARTIN MARIETTA

Tokamak Confinement Projections and Performance Goals

N. A. Uckan

OAK RIDGE NATIONAL LABORATORY
CENTRAL RESEARCH LIBRARY
CIRCULATION SECTION
4500N ROOM 175
LIBRARY LOAN COPY
DO NOT TRANSFER TO ANOTHER PERSON
If you wish someone else to see this report, send in name with report and the library will arrange a loan.

OPERATED BY
MARTIN MARIETTA ENERGY SYSTEMS, INC.
FOR THE UNITED STATES
DEPARTMENT OF ENERGY

Printed in the United States of America. Available from
National Technical Information Service
U.S. Department of Commerce
5285 Port Royal Road, Springfield, Virginia 22161
NTIS Price Codes: Printed Copy: A03; Microfiche A01

This report was prepared as an account of work sponsored by an agency of the United States Government. Neither the United States Government nor any agency thereof, nor any of their employees, makes any warranty, express or implied, or assumes any legal liability or responsibility for the accuracy, completeness, or usefulness of any information, apparatus, product, or process disclosed, or represents that its use would not infringe privately owned rights. Reference herein to any specific commercial product, process, or service by trade name, trademark, manufacturer, or otherwise, does not necessarily constitute or imply its endorsement, recommendation, or favoring by the United States Government or any agency thereof. The views and opinions of authors expressed herein do not necessarily state or reflect those of the United States Government or any agency thereof.

ORNL/TM-10854
Dist. Category UC-420

Fusion Energy Division

TOKAMAK CONFINEMENT PROJECTIONS AND PERFORMANCE GOALS

N. A. Uckan

Presented at the 8th Topical Meeting on the Technology of Fusion Energy,
Salt Lake City, Utah, October 9–13, 1988

Date Published: November 1988

Prepared by the
OAK RIDGE NATIONAL LABORATORY
Oak Ridge, Tennessee 37831
operated by
MARTIN MARIETTA ENERGY SYSTEMS, INC.
for the
U.S. DEPARTMENT OF ENERGY
under contract DE-AC05-84OR21400

MARTIN MARIETTA ENERGY SYSTEMS LIBRARIES
3 4456 0284113 8

CONTENTS

ABSTRACT v
1. INTRODUCTION 1
2. PERFORMANCE GOALS AND FIGURES OF MERIT 1
3. CONFINEMENT PROJECTIONS 6
APPENDIX 10
REFERENCES 12

ABSTRACT

One key quantity to be determined in the design of burning-plasma devices (CIT, ITER, reactors, etc.) is the level of plasma current (I) required to meet the desired plasma performance goals (ignition, high Q, etc.) and device objectives (fusion power, wall loading, current drive power, etc.). It is shown that these goals and objectives can be expressed in terms of the "figure-of-merit" parameter IA^{α}/R^{x} [$\sim f(LB^{y})$], where A is the aspect ratio, R is the major radius, L ($= R, a$) is the characteristic length, B is the toroidal magnetic field on axis, and the exponents $\alpha \sim 1 \pm 0.5$ and $x \sim 0$–0.5 ($y \sim 1$–2) depend on the confinement assumptions and operational limits. To reach ignition or high Q, the main goal is to optimize IA^{α}/R^{x}, subject to other engineering design constraints. In a CIT-like device (with $R \sim 2$ m, $\kappa \sim 2$, $q_{\psi} \geq 3$), the ignition requirement is $I(A/3)^{\alpha} \sim 9$–15 MA for "enhanced" L-mode (H-mode) confinement scaling expressions; an ITER-like device (with $R \sim 5$–6 m, $\kappa \sim 2$, $q_{\psi} \geq 3$) would require $I(A/3)^{\alpha} \sim 15$–25 MA. These requirements are embodied in the present CIT (with $I \sim 11$ MA, $A \sim 3.25$) and ITER (with $I \sim 18$–22, $A \sim 3.1$–2.6) designs.

1. INTRODUCTION

Energy confinement is a major issue for the next-generation, burning-plasma devices [Compact Ignition Tokamak[1] (CIT), International Thermonuclear Experimental Reactor[2] (ITER), etc.]. The physics of energy transport in tokamaks is not yet fully understood. Therefore, the energy confinement time in these burning-plasma devices has to be estimated from extrapolations of the available experimental data base by using empirically developed scaling expressions[3] as well as scalings derived from various theoretical models[4] for the dominant transport mechanisms. The selection of a particular scaling or transport model has a large impact on the design and parameter choices. Thus, the identification and formulation of "figure-of-merit" parameters such as $Tn\tau_E \propto f(IA^{\alpha}/R^{x}) \propto f(LB^{y})$ are useful in guiding the design efforts to optimize energy confinement and to establish trade-offs between plasma size ($L = a, R$), current (I), field (B), aspect ratio (A), etc. In this paper we formulate these figure-of-merit parameters and assess the confinement capabilities of CIT and ITER.

Unless otherwise stated, all units are mks, with T in keV, I in MA, and power in MW.

2. PERFORMANCE GOALS AND FIGURES OF MERIT

There are several performance indicators for tokamaks; the level of plasma current (I) is one of the most important because of the favorable scaling of confinement time τ_E and limits on plasma beta β_{crit} and density $\langle n\rangle_{max}$ with increasing I. One key quantity to be determined in the design of CIT and ITER (or any burning-plasma devices) is the level of plasma current required to meet the desired plasma performance goals ($Tn\tau_E$ – ignition, high Q, etc.) and machine objectives (fusion power P_{fus}, wall loading Γ_w, current drive power P_{CD}, etc.).

Here we define a fusion-related parameter

$$T_{10}n_{20}\tau_E = \langle T/10\ \text{keV}\rangle\langle n_e/10^{20}\ \text{m}^{-3}\rangle\tau_E$$

where $\langle n_e \rangle$ is the volume-averaged electron density and $\langle T \rangle$ is the density-weighted average temperature ($T_i \approx T_e \approx T$). The importance of this parameter derives from the fact that, in the temperature range $7 < T < 20$ keV, the D-T fusion reaction rate coefficient $\langle \sigma v \rangle \propto T^2$, and a measure of confinement capability $M \propto P_\alpha / P_{loss} \propto T_{10} n_{20} \tau_E$, where P_α is the total alpha power and $P_{loss} = P_{cond} + P_{rad}$ is the power lost by conduction and radiation. For relatively broad (square-root parabolic density and parabolic temperature) profiles with $Z_{eff} \sim 1.5$ (5% thermal alphas plus carbon and oxygen impurities), the ignition requirement[5] is $T_{10} n_{20} \tau_E \sim 3 \pm 0.3$ for $\langle T \rangle \sim 7$–20 keV. With a Murakami-Hugill ($n_{mu} \sim 1.5B/Rq_*$) or Greenwald ($n_{gr} \sim 0.27I/a^2$) type limit for density, the Troyon limit for beta [$\beta_{crit} \sim CI/aB$, $C \sim (2.5$–$3)\%$], and $q_\psi > 3$–3.5 for MHD stability, the optimum temperature for ignition is typically $\sim 10 \pm 2$ keV for many of the confinement scaling models.[3–11]

For a wide range of (ohmic or auxiliary heating) confinement scaling models of the form τ_{EOH}(neo-Alcator) $\propto nL^3$ and/or τ_{Eaux}(L-/H-mode) $\propto LIf(P)$ with $f(P) \sim P^{-\gamma}$ or $\sim (C_1 + C_2/P)$, $Tn\tau_E \propto f(IA^\alpha/R^x)$. An example of the power law form of τ_E is the Goldston scaling[6]

$$\tau_E = \tau_G = 0.037IP^{-0.5}R^{1.75}a^{-0.37}\kappa^{0.5}(A_i/1.5)^{0.5}$$

$$T_{10}n_{20}\tau_E = 2.53 \times 10^{-4}(IA^{1.37}/R^{0.12})^2$$

where $A_i \approx 2.5$ is the average atomic mass and $P = W/\tau_E = P_{aux} + P_{OH} + P_\alpha - P_{rad} \approx 9n_{20}T_{10}Ra^2\kappa/\tau_E$ is the net heating power. An example of the offset linear form is the Rebut-Lallia scaling[10]

$$\tau_E = \tau_{RL} = C_R I l^{1.5} + C_L n_{20}^{0.75} I^{0.5} B^{0.5} l^{2.75}/P$$

$$T_{10}n_{20}\tau_E \propto I^3A^2/R^{0.5} \propto (IA^{0.67}/R^{0.17})^3$$

where $l = (Ra^2\kappa)^{1/3}$, $C_R = (0.024/Z_{eff}^{0.5})(A_i/2)^{0.5}$, $C_L = 0.29Z_{eff}^{0.25}(A_i/2)^{0.5}$, and $Tn\tau_E$ is evaluated at the beta limit ($\propto I/aB$).

Table I lists [for a given plasma shape (κ, δ) and q_ψ] the ignition/burn-related plasma performance goals in terms of the figure-of-merit parameter IA^α/R^x for a number of confinement scaling expressions (see Appendix), evaluated at the density ($n \propto I/a^2$) and beta ($\beta \propto I/aB$) limits. Also listed are the scalings of Q, P_{fus}, Γ_w, and P_{CD}. The lower bound on IA^α/R^x, in terms of confinement, is set by the containment of alpha particles ($\alpha = 0.5$, $x = 0$) and by the irreducible neoclassical transport ($\alpha = 3/8$, $x = 0$). All of the scalings show a weaker dependence on size ($x \sim 0.1$–0.5). Power law scalings[3,6–8] (Goldston, Kaye-Goldston, Kaye, T-10, etc.) exhibit a stronger dependence on aspect ratio ($\alpha \sim 0.8$–1.5) than the offset linear forms[9–11] (Odajima-Shimomura, Rebut-Lallia, etc.), where $\alpha \leq 0.5$. A simple overall average scaling is $\langle\alpha\rangle \sim 1.1$, $\langle x\rangle \sim 0.4$, which can be used as a reasonable measure of confinement capability for designs with $A \sim 2.5$–4. It should be noted that the results presented here should not be extrapolated to very high aspect ratios because the scaling of confinement with A is one of the most uncertain elements of the present experimental data base.

As an example, with $n \approx n_{mu}$ and $\langle T\rangle \approx 10$ keV, Fig. 1 shows the normalized current $[I(A/3)^\alpha]$ needed for ignition as a function of plasma size (R or a) for some of the confinement scalings given in Table I for fixed plasma shape ($\kappa = 2$, $\delta = 0.4$), safety factor ($q_\psi \approx 3$–3.5), and $Z_{eff} \approx 1.5$. Because the neo-Alcator (NA) scaling represents an upper limit to confinement, in Fig. 1 we have used a combined form for τ_E, taken as $\tau_E = [(\tau_{NA})^2 + (\tau_{aux})^2]^{-1/2}$, where aux represents the additional scaling used (G, KG, etc.). It is also possible to consider $\tau_E = \min(\tau_{NA}; \tau_{aux})$. Results from detailed analysis (and Fig. 1) indicate that, for a CIT-size device (with $R \sim 2$ m, $\kappa = 2$, $\delta = 0.4$, $q_\psi \approx 3$–3.5) the ignition requirement is $I(A/3)^\alpha \sim 9$–15 MA for H-mode or enhanced L-mode scalings, where τ_E(H-mode) $= f \times \tau_E$(L-mode) with an enhancement factor $f \geq 1.4$–2. For an ITER-size device (with $R \sim 5$–6 m), $I(A/3)^\alpha \sim 15$–25 MA is required for ignition. A similar-size ITER with noninductive current drive and a wall loading of $\Gamma_w \sim 1$ MW/m^2 would require $I(A/3) \sim 14$–17 MA, in which $Q \sim 5$–10 operation is possible for various current drive schemes[12] (with varying bootstrap contribution, 0–30%) requiring current drive (absorbed) power of $P_{CD} \sim 75$–150 MW.

TABLE I.
Current, Size, and Aspect Ratio Scaling of
Confinement Capability
[Evaluated at n or β limit; with fixed $\langle T \rangle$ and (q, κ, δ)]

Confinement scaling[3–11]		$Tn\tau_E \sim f[(IA^{\alpha}/R^{x})^{z}]$ At n limit	At β limit
NC	Neoclassical	$(IA^{3/8}/R^{0})^{2}$	$(IA^{3/8}/R^{0})^{2}$
NA	Neo-Alcator (OH)	$(IA^{1.5}/R^{0.5})^{2}$	$(IA^{1.25}/R^{0.25})^{4}$
G	Goldston	$(IA^{1.37}/R^{0.12})^{2}$	$(IA^{1.37}/R^{0.12})^{2}$
KG	Kaye-Goldston	$(IA^{1.32}/R^{0.55})^{3}$	$(IA^{1.3}/R^{0.5})^{3.2}$
KA	Kaye (All)	$(IA^{1.2}/R^{0.68})^{2.5}$	$(IA^{1.2}/R^{0.63})^{2.7}$
KB	Kaye (Big)	$(IA^{0.8}/R^{0.56})^{2.5}$	$(IA^{0.82}/R^{0.52})^{2.7}$
T10	T-10	$(IA^{1.5}/R^{0.5})^{2.53}$	$(IA^{1.44}/R^{0.44})^{2.87}$
OS	Odajima-Shimomura	(IA^{0}/R^{0})	$(IA^{0.5}/R^{0})^{2}$
RL	Rebut-Lallia	$(IA^{0.5}/R^{0.25})^{2}$	$(IA^{0.67}/R^{0.17})^{3}$
AX	ASDEX-H	$(IA/R^{0.56})^{2}$	$(IA/R^{0.33})^{3}$
"Simple Average"		$(IA^{1.1}/R^{0.4})^{2.15}$	$(IA^{1.1}/R^{0.3})^{2.75}$
		$[\langle \alpha \rangle \sim 1.1; \langle x \rangle \sim 0.35; \langle z \rangle \sim 2.45]$	
Q	Energy gain factor	$(IA/R^{0})^{0}$	$(IA/R^{0})^{1.0}$
Γ_w	Wall loading	$(IA^{1.5}/R^{1.5})^{2}$	$(IA^{1.25}/R^{0.75})^{4}$
P_{fus}	Fusion power	$(IA/R^{0.5})^{2}$	$(IA/R^{0.25})^{4}$
P_{CD}	Current drive power	$(IA/R^{0.5})^{2}$	$(IA/R^{0.33})^{3}$

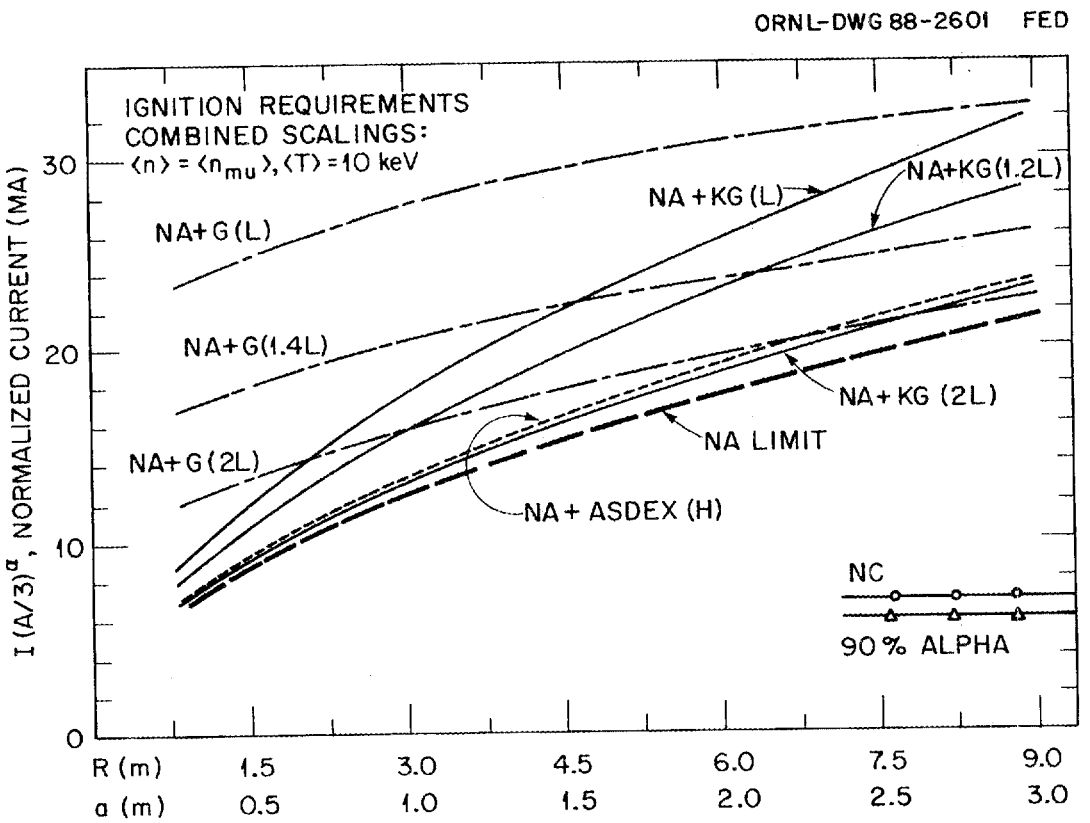

Fig. 1. Plasma current $[I(A/3)^{\alpha}]$ required for ignition vs size (R, a) for various confinement scalings (combined with neo-Alcator) for fixed plasma shape ($\kappa = 2$, $\delta = 0.4$) and $q_{\psi} \approx 3$–3.5, evaluated at ($n \sim n_{mu}$, $T \sim 10$ keV) (see Table I for notations).

3. CONFINEMENT PROJECTIONS

A detailed assessment of confinement projections for CIT and ITER has been carried out. The evaluation was based mainly on consideration of various empirical scaling expressions deduced from experiments, although theoretical models were also considered. Table II lists the representative device parameters for CIT and several ITER options and compares the confinement capabilities in terms of the figure of merit parameter IA^{α}/R^{x}. In Table II, the three ITER options represent the range of machines studied by the ITER design team at Garching.[2] ITER-0 (5.8 m, 20 MA) is the machine initially used to scope out physics and engineering issues. Recently, the ITER design team picked a machine with two operating phases: technology phase (ITER-1: 5.5 m, 18 MA) and physics phase (ITER-2: 5.8 m, 22–25^{+} MA). Although there are slight differences in physics design guidelines and assumptions for CIT and ITER, for comparison purposes and uniformity we use a common set of physics models and assumptions ($Z_{eff} \approx 1.5$ with $n_{\alpha}/n_{e} \approx 5\%$, $\beta_{crit} \sim 3I/aB$, etc.).

As seen from Table II, all ITER versions have comparable performance, except for extended capability in the physics phase (ITER-2 with 25 MA) in which the performance is better. Here the performance is measured by relative magnitudes of the figure-of-merit parameter (IA^{α}/R^{x}). On the average, CIT and ITER confinement capabilities are also comparable; however, there are marked differences with respect to power law and offset linear forms of scalings. For the offset linear form (Rebut-Lallia, Odajima-Shimomura, etc.), performance is better in ITER (by as much as 50%) than in CIT. With Kaye-type scalings[3,7] (IA^{α}/R^{x} with $\alpha \sim 0.8$–1.3, $x \sim 0.5$), CIT exhibits a slightly better performance; large current in ITER is balanced with compact size and somewhat higher A in CIT. With the Goldston scaling, ITER performs better due to large current and weak size scaling.

Table III summarizes the CIT and ITER ignition requirements for various scaling expressions. Given in the table are the minimum L-mode enhancement factors needed for ignition, evaluated at the beta limit (and $T \sim 10$ keV) assuming broad (a squareroot parabolic density and a parabolic temperature) profiles and $Z_{eff} \approx 1.5$ with $n_{\alpha}/n_{e} \approx 5\%$.

Table II.
Representative CIT and ITER Parameters and Confinement Capabilities

Design Parameters[1,2]

	CIT	ITER-0	ITER-1	ITER-2
R (m)	2.1	5.8	5.5	5.8
a (m)	0.65	2.0	1.8	2.2
$A = R/a$	3.25	2.9	3.1	2.6
κ (at 95% flux)	2	2	1.9	1.9
δ (at 95% flux)	0.4	0.4	0.4	0.4
B_0 (T)	10	5.1	5.3	5.0
I (MA)	11	20	18	22–25
Calculated Parameters and Confinement Capability				
q_* (at 95%)	2.7	2.6	2.4	2.6–2.3
q_ψ (at 95%)	3.2	3.2	2.85	3.2–2.9
Troyon beta limit (%)				
$\beta_{crit} = 3I/aB_0$	5.1	5.9	5.65	6–6.8
$= 2.5I/aB_0$	4.2	4.9	4.7	5–5.7
Density limit (10^{20} m^{-3})				
$\langle n_{mu}\rangle \approx 1.5B_0/Rq_*$	2.6	0.5	0.6	0.5–0.6
$\langle n_{gr}\rangle \approx 0.27I/a^2$	7.0	1.35	1.5	1.2–1.4
$\langle n(\text{at } \beta_{crit}, 10 \text{ keV})\rangle$	5.9	1.8	1.85	1.7–2.0
Figure of merit (at β limit)				
<Average>: $IA/R^{0.3}$	29	34	33	34–39
G: $IA^{1.37}/R^{0.12}$	50.5	69.5	68	67–76
KG: $IA^{1.3}/R^{0.5}$	35	33	33	32–37
KA: $IA^{1.2}/R^{0.63}$	28	24	23.5	23–26
KB: $IA^{0.82}/R^{0.52}$	19.5	19	18.5	19–22
RL: $IA^{0.67}/R^{0.17}$	21	30	28.5	31–35
OS: $IA^{0.5}/R^{0}$	20	34	31	36–41

Table III.
CIT and ITER Ignition Capability:
L-mode Enhancement Factor (f) Needed for Ignition
for Various Confinement Scalings[3–11]
(Evaluated at Beta Limit $\beta \sim 3I/aB$ %, fixed T)[a]

Confinement scaling		CIT 11 MA	ITER-0 20 MA	ITER-1 18 MA	ITER-2 22 MA
NA	Neo-Alcator	Ignited	Ignited	Ignited	Ignited
AX	ASDEX-H	Ignited	Ignited	Ignited	Ignited
G	Goldston	>2.1	>1.6	>1.6	>1.6
KA	Kaye ("all")	>1.8	>2.3	>2.3	>2.3
KB	Kaye ("big")	>1.9	>2	>2	>1.9
T-10	T-10	>1.6	>1.6	>1.6	>1.6
OS	Odajima-Shimomura	>2.4	>1.3	>1.5	>1.2
RL	Rebut-Lallia	>1.1	Ignited	Ignited	Ignited

[a] $\tau_E = \min(\tau_{NA}; \tau_{aux})$, aux = G, KA, KB, T-10, OS, RL

For CIT, the predictions (see Table III) with Goldston and Odajima-Shimomura scalings are the most pessimistic ($f \sim 2.1$–2.3), followed by the recent Kaye ("all" and "big") scalings[3] ($f \sim 1.8$–1.9). Ignition with L-mode is nearly accessible with the optimistic Rebut-Lallia scaling ($f \sim 1.1$). For ITER, the most pessimistic performance is with the recent Kaye (all and big) scaling expressions ($f \sim 1.9$–2.3), whereas the best performance is with the offset linear forms (Rebut-Lallia ignition with L-mode and Odajima-Shimomura requires $f \sim 1.2$–1.5). Projections with the T-10 scaling are uniform across the board, $f \sim 1.6$ for both the CIT and the ITERs.

For the most part, attainment of ignition in both CIT and ITER relies mostly on the attainment of an enhancement (H-mode) over the L-mode confinement. With marginal or poor confinement (i.e., saturated ohmic and most L-mode scalings), ignition probability is very low and access to high-Q operation depends sensitively on the available auxiliary power (P_{aux}), which may be too large to be practical. The minimum auxiliary power requirement is obtained from the saddle point (n_*,T_*) equation. For a confinement model of the form $\tau_E \sim n^x T^y f(\text{others})$, where f(others) contains the dependence of τ_E on parameters other than n and T, the saddle point equation is[5]

$$
\begin{aligned}
[(1 + x)/2]P_{cond} &= P_{aux} + P_{OH} \\
[(1 - x)/2]P_{cond} &= P_{\alpha} + P_{rad} \\
(1 - y)P_{cond} &= 2\,P_{\alpha} - 1.5\,P_{OH} - 0.5\,P_{rad}
\end{aligned}
$$

where $\langle\sigma v\rangle \sim T^2$ is assumed (valid for $T \sim 7$–20 keV). Solutions to these equations give the density and temperature at the saddle point (n_*,T_*) and the required minimum P_{aux}(max). The simplest, although one of the more pessimistic, of the examples is one with τ_E = constant (i.e., x = y = 0). For reference density and temperature profiles (α_n = 0.5 and α_T = 1.0),

$$\min P_{aux}(n_*,T_*) \approx (s_1/\tau_E - s_2)V\ (\text{MW})$$

$$\beta(n_*,T_*) \approx 1.68 s_1/B^2$$

where V is the plasma volume, $s_1 \approx 5.6 \times 10^{-2}(I/\kappa a^2)$, and $s_2 \approx 0.85 s_1^2$.

The ignition capability can be significantly improved with centrally peaked density and heat deposition profiles. A centrally peaked density profile leads to an enhanced fusion rate and therefore a greater margin against confinement losses. Although it may be possible to maintain peak profiles transiently in CIT (which operates for short pulses), attainment and sustainment of such peaked profiles over longer periods in ITER-like (long-pulse, steady-state) plasmas may not be compatible with the MHD stability and H-mode-like conditions needed for good confinement.

APPENDIX

CONFINEMENT SCALING EXPRESSIONS

1. Neo-Alcator (NA) OH scaling:

$$\tau_{NA} = 0.07 n_{20} a R_o^2 q_*$$

where q_* is the cylindrical equivalent safety factor[5]

$$q_* \approx (5a^2 B_o / R_o I)[1 + \kappa^2(1 + 2\delta^2 - 1.2\delta^3)]/2$$

2. Goldston (G) L-mode scaling:[6]

$$\tau_G = 0.037 I P^{-0.5} R_o^{1.75} a^{-0.37} \kappa^{0.5} (A_i/1.5)^{0.5}$$

where P is the "net" heating power

$$P = W/\tau_E = 0.24\, n_{20} T_{10} (1 + n_i/n_e)\, V/\tau_E = P_{aux} + P_{OH} + P_\alpha - P_{rad}$$

(For $Z_{eff} \approx 1.5$, $P \approx 9 n_{20} T_{10} a^2 R \kappa / \tau_E$.)

3. Kaye-Goldston (KG) L-mode scaling:[7]

$$\tau_{KG} = 0.055 I^{1.24} P^{-0.58} R_o^{1.65} a^{-0.49} \kappa^{0.28} n_{20}^{0.26} B_o^{-0.09} (A_i/1.5)^{0.5}$$

4. Kaye "all" (KA) L-mode scaling:[3]

$$\tau_{KA} = 0.067 I^{0.85} P^{-0.5} R_o^{0.85} a^{0.3} \kappa^{0.25} n_{20}^{0.1} B_o^{0.3} A_i^{0.5}$$

5. Kaye "big" (KB) L-mode scaling:[3]

$$\tau_{KB} = 0.105 I^{0.85} P^{-0.5} R_o^{0.5} a^{0.8} \kappa^{0.25} n_{20}^{0.1} B_o^{0.3} A_i^{0.5}$$

6. T-10 L-mode scaling:[8]

$$\tau_{T\text{-}10} \approx 0.095 a R_o B_o \kappa^{0.5} P^{-0.4} [Z_{eff}^2 I^4 / (a R q_*^3 \kappa^{1.5})]^{0.08}$$

7. JAERI or Odajima-Shimomura (OS) L-mode scaling:[9]

$$\tau_{OS} = [0.085\kappa a^2 + 0.069 I n_{20}^{0.6} B_o^{0.2} R_o^{1.6} a^{0.4} \kappa^{0.2} G(q_*, Z_{eff})/P]\, A_i^{0.5}$$

where

$$G(q_*, Z_{eff}) = Z_{eff}^{0.4}[(15 - Z_{eff})/20]^{0.6}[3q_*(q_* + 5)/(q_* + 2)(q_* + 7)]^{0.6}$$

8. Rebut-Lallia (RL) L-mode scaling:[10]

$$\tau_{RL} = [0.024 I l^{1.5}/Z_{eff}^{0.5} + 0.29 n_{20}^{0.75} I^{0.5} B_o^{0.5} l^{2.75} Z_{eff}^{0.25}/P](A_i/2)^{0.5}$$

where $l = (R_o a^2 \kappa)^{1/3}$ is the characteristic scale length.

9. ASDEX (AX) H-mode scaling:[11]

$$\tau_{AXH} = 0.1 I R_o$$

In all expressions, the units are mks with current in MA, powers in MW, temperatures in keV, with κ and δ at 95% flux and

n_{20} $= \langle n_e \rangle / 10^{20}$ m^{-3}
= volume-averaged electron density,

T_{10} $= \langle T \rangle / 10$ keV
= density-weighted average temperature,

q_ψ $\approx q_* f(\varepsilon) \approx q_* [(1.77 - 0.65\varepsilon)/(1 - \varepsilon^2)^2]$; $\varepsilon = a/R_o$
= MHD safety factor,

A_i = average atomic mass $\approx$ 2.5 for a 50:50 D-T plasma,

Z_{eff} = effective charge $\approx$ 1.5 (assumed for this study),

P $= W/\tau_E = 0.24\, n_{20}\, T_{10}\, (1 + n_i/n_e)\, V/\tau_E$
$= P_{aux} + P_{OH} + P_\alpha - P_{rad}$
= "net heating" power.

Profiles: $n,T \sim (1 - r^2/a^2)^{\alpha_{n,T}}$, $\alpha_n = 0.5$ and $\alpha_T = 1.0$.

REFERENCES

1. D. J. GROVE, "Current Status and Design of the CIT," to appear in Proc. *8th Topical Meeting on the Technology of Fusion Energy*, Salt Lake City, Utah, October 9–13, 1988; R. PARKER et al., "CIT Physics Design Description," AE-880112-PPl-01, Princeton Plasma Physics Laboratory (1988); D. POST et al., "Physics Aspects of the Compact Ignition Tokamak," *Phys. Scr.*, **T16**, 89 (1987).
2. "ITER Definition Phase Report," International Atomic Energy Agency, Vienna (to be published); ITER Physics Team (presented by D. POST), "ITER: Physics Basis," paper IAEA-CN-50/F-II-1, to appear in *Proc. 12th Int. Conf. Plasma Physics and Controlled Nuclear Fusion Research*, Nice, France, October 12–19, 1988.
3. For review of empirical scaling expressions, see S. M. KAYE, "Survey of Energy Confinement Scaling Expressions," *ITER Specialists' Meeting on Energy Confinement*, May 24–27, 1988, Garching, Federal Republic of Germany.
4. For review of theoretical models, see J. D. CALLEN, "Overview of Confinement Theory," *ITER Specialists' Meeting on Energy Confinement*, May 24–27, 1988, Garching, Federal Republic of Germany.
5. N. A. UCKAN, "Relative Merits of Size, Field, and Current on Ignited Tokamak Performance," *Fusion Technol.*, **14**, 299 (1988); N. A. UCKAN and J. SHEFFIELD, "A Simple Procedure for Establishing Ignition Conditions in Tokamaks," *Tokamak Startup*, p. 45, H. Knoepfel, Ed., Plenum Press, New York (1986).
6. R. J. GOLDSTON, "Energy Confinement Scaling in Tokamaks," *Plasma Phys. Controlled Fusion*, **26**, 87 (1984).
7. S. M. KAYE and R. J. GOLDSTON, "Global Energy Confinement Scaling of Neutral Beam Heated Tokamaks," *Nucl. Fusion*, **25**, 65 (1985).
8. T-10 GROUP, "Investigation of Energy Confinement in ECH Experiments on T-10," *ITER Specialists' Meeting on Energy Confinement*, May 24–27, 1988, Garching, Federal Republic of Germany.
9. K. ODAJIMA and Y. SHIMOMURA, "Energy Confinement Scaling Based on Offset Linear Characteristics," JAERI Report, JAERI-M 88-068 (March 1988).
10. P. H. REBUT, P. P. LALLIA, and M. L. WATKINS, "Chaotic Magnetic Topology and Heat Transport in Tokamaks," JET Report, JET-P(88)05 (January 1988, corrigendum March 1988).
11. O. GRUBER, "Confinement Regimes in Ohmically and Auxiliary Heated Tokamaks," *Proc. Int. Conf. Plasma Physics*, Lausanne, Switzerland, June 27-July 3, 1984, Vol. 1, p. 67, Commission of the European Communities (1984).
12. For an overview, see N. J. FISCH, "Theory of Current Drive in Plasmas," *Rev. Mod. Phys.*, **59**, 175 (1987).

ORNL/TM-10854
Dist. Category UC-420

INTERNAL DISTRIBUTION

1. L. A. Berry
2. R. A. Dory
3. J. L. Dunlap
4. J. D. Galambos
5. J. T. Hogan
6. W. A. Houlberg
7. Y-K. M. Peng
8. R. L. Reid
9. M. J. Saltmarsh
10. T. E. Shannon
11. J. Sheffield

12–16. N. A. Uckan

17. T. Uckan

18–19. Laboratory Records Department

20. Laboratory Records, ORNL-RC
21. Document Reference Section
22. Central Research Library
23. Fusion Energy Division Library

24–25. Fusion Energy Division Publications Office

26. ORNL Patent Office

EXTERNAL DISTRIBUTION

27. M. A. Abdou, School of Engineering and Applied Science, 6288 Boelter Hall, University of California Los Angeles, Los Angeles, CA 90024
28. C. C. Baker, Argonne National Laboratory, Fusion Power Program, Bldg. 205, 9700 South Cass Avenue, Argonne, IL 60439
29. G. Bateman, Plasma Physics Laboratory, Princeton University, P.O. Box 451, Princeton, NJ 08543
30. C. Bolton, Office of Fusion Energy, Office of Energy Research, Germantown ER-55, U.S. Department of Energy, Washington, DC 20545
31. K. Borrass, NET Team, Max-Planck-Institut, Boltzmannstrasse 2, D-8046 Garching bei Muenchen, Federal Republic of Germany
32. J. D. Callen, Department of Nuclear Engineering, University of Wisconsin, Engineering Research Building, 1500 Johnson Drive, Madison, WI 53706
33. D. R. Cohn, 167 Albany St., NW 16-140, Massachusetts Institute of Technology, Cambridge, MA 02139
34. R. W. Conn, Fusion Engineering and Physics Program, 6291 Boelter Hall, University of California Los Angeles, Los Angeles, CA 90024

35. B. Coppi, 77 Massachusetts Avenue, 26-217, Massachusetts Institute of Technology, Cambridge, MA 02139
36. D. H. Crandall, Office of Fusion Energy, Office of Energy Research, Germantown ER-542, U.S. Department of Energy, Washington, DC 20545
37. R. C. Davidson, 77 Massachusetts Avenue, Massachusetts Institute of Technology, Cambridge, MA 02139
38. N. A. Davies, Office of Fusion Energy, Office of Energy Research, Germantown ER-55, U.S. Department of Energy, Washington, DC 20545
39. S. O. Dean, Fusion Power Associates, 2 Professional Drive, Suite 249, Gaithersburg, MD 20760
40. S. R. DeVoto, Lawrence Livermore National Laboratory, P.O. Box 5511, Livermore, CA 94550
41. S. A. Eckstrand, Office of Fusion Energy, Office of Energy Research, Germantown ER-55, U.S. Department of Energy, Washington, DC 20545
42. G. A. Eliseev, I. V. Kurchatov Institute of Atomic Energy, Ploshchad' Akademika Kurchatova 46, Moscow 123182, U.S.S.R.
43. F. Engelmann, NET/ITER Team, Max-Planck-Institut, Boltzmannstrasse 2, D-8046 Garching bei Muenchen, Federal Republic of Germany
44. A. J. Favale, Grumman Aerospace Corporation, MS-A0126, P.O. Box 31, Bethpage, NY 11714
45. H. K. Forsen, Bechtel Group Inc., Research and Engineering, P.O. Box 3965, San Francisco, CA 94119
46. T. K. Fowler, Department of Nuclear Engineering, University of California Berkeley, Etcheverry Hall Room 4153, Berkeley, CA 94720
47. N. Fujisawa, Naka Fusion Research Establishment, Japan Atomic Energy Research Inst., Naka-Machi, Naka-Gun, Ibaraki-ken 311-02, Japan
48. H. P. Furth, Plasma Physics Laboratory, Princeton University, P.O. Box 451, Princeton, NJ 08543
49. J. R. Gilleland, Lawrence Livermore National Laboratory, P.O. Box 5511, Livermore, CA 94550
50. R. J. Goldston, Plasma Physics Laboratory, Princeton University, P.O. Box 451, Princeton, NJ 08543
51. R. W. Gould, Department of Applied Physics, California Institute of Technology, Pasadena CA 91125
52. R. A. Gross, Plasma Resesarch Laboratory, Columbia University, New York, NY 10027
53. C. D. Henning, Lawrence Livermore National Laboratory, P.O. Box 5511, Livermore, CA 94550

54. T. R. James, Office of Fusion Energy, Office of Energy Research, Germantown ER-55, U.S. Department of Energy, Washington, DC 20545
55. R. A. Krakowski, CTR-12, Mail Stop 641, Los Alamos National Laboratory, P.O. Box 1663, Los Alamos, NM 87545
56. G. L. Kulcinski, Department of Nuclear Engineering, University of Wisconsin, Engineering Research Building, 1500 Johnson Drive, Madison, WI 53706
57. B. G. Logan, Lawrence Livermore National Laboratory, P.O. Box 5511, Livermore, CA 94550
58. D. M. Meade, Plasma Physics Laboratory, Princeton University, P.O. Box 451, Princeton, NJ 08543
59. G. H. Miley, Fusion Studies Laboratory, University of Illinois, 214 Nuclear Engineering Laboratory, 103 S. Goodwin Ave., Urbana, IL 61801
60. V. Mukhovatov, I. V. Kurchatov Institute of Atomic Energy, 46 Ulitsa Kurchatova, P.O. Box 3402, Moscow 123182, U.S.S.R.
61. W. M. Nevins, Lawrence Livermore National Laboratory, P.O. Box 5511, Livermore, CA 94550
62. A. Opdenaker, Office of Fusion Energy, Office of Energy Research, Germantown ER-532, U.S. Department of Energy, Washington, DC 20545
63. R. R. Parker, Plasma Fusion Center, Massachusetts Institute of Technology, Cambridge, MA 02139
64. D. E. Post, Plasma Physics Laboratory, Princeton University, P.O. Box 451, Princeton, NJ 08543
65. F. Prevot, Association EURATOM-CEA, Depertament de Recherches sur la Fusion Controlee, Centre d'Etudes Nucleaires de Cadarache, 13108 Saint Paul Lez Durance Cedex, Cadarache, France
66. S. Putvinskji, I. V. Kurchatov Institute of Atomic Energy, 46 Ulitsa Kurchatova, P.O. Box 3402, Moscow 123182, U.S.S.R.
67. P. H. Rebut, JET Joint Undertaking, Abingdon, Oxon, OX14 3EA, England
68. F. L. Ribe, College of Engineering, FL-10, AERL Bldg., University of Washington, Seattle, WA 98195
69. P. H. Rutherford, Plasma Physics Laboratory, Princeton University, P.O. Box 451, Princeton, NJ 08543
70. W. L. Sadowski, Office of Fusion Energy, Office of Energy Research, Germantown ER-541, U.S. Department of Energy, Washington, DC 20545
71. J. A. Schmidt, Plasma Physics Laboratory, Princeton University, P.O. Box 451, Princeton, NJ 08543
72. C. F. Singer, Fusion Studies Laboratory, University of Illinois, 214 Nuclear Engineering Laboratory, 103 S. Goodwin Ave., Urbana, IL 61801

73. W. M. Stacey, Jr., Georgia Institute of Technology, Fusion Research Center, Atlanta, GA 30332
74. R. D. Stambaugh, General Atomics, P.O. Box 85608, San Diego, CA 92138
75. D. Steiner, Rensselaer Polytechnic Institute, Department of Nuclear Engineering, Troy, NY 12181
76. M. Sugihara, Naka Fusion Research Establishment, Japan Atomic Energy Research Institute, Naka-Machi, Naka-Gun, Ibaraki-ken 311-02, Japan
77. V. T. Tolok, Kharkov Physical-Technical Institute, Academical St. 1, 310108 Karkov, U.S.S.R.
78. V. Varma, Physical Research Laboratory, Navrangpura, Ahmedabad, India
79. H. Weitzner, Courant Institute of Mathematical Sciences, New York University, 251 Mercer Street, New York, NY 10012
80. J. W. Willis, Office of Fusion Energy, Office of Energy Research, Germantown ER-55, U.S. Department of Energy, Washington, DC 20545
81. Bibliothek, Max-Planck-Institut fur Plasmaphysik, Boltzmannstrasse 2, D-8046 Garching bei Muenchen, Federal Republic of Germany
82. Bibliothek, Institut fur Plasmaphysik, KFA Julich GmbH, Postfach 1913, D-5170 Julich, Federal Republic of Germany
83. Bibliothek, KfK Karlsruhe GmbH, Postfach 3640, D-7500 Karlsruhe 1, Federal Republic of Germany
84. Bibliotheque, Service du Confinement des Plasmas, CEA, B.P. No. 6, 92 Fontenay-aux-Roses (Seine), France
85. Bibliotheque, Association EURATOM-CEA, Depertament de Recherches sur la Fusion Controlee, Centre d'Etudes Nucleaires de Cadarache, F-13108 Saint Paul Lez Durance Cedex, Cadarache, France
86. Documentation S.I.G.N., Departement de la Physique du Plasma et de la Fusion Controlee, Association EURATOM-CEA, Centre d'Etudes Nucleaires, B.P. 85, Centre du Tri, F-38041 Grenoble, France
87. Bibliotheque, Centre de Recherches en Physique des Plasmas, Ecole Polytechnique Federale de Lausanne, 21 Avenue des Bains, CH-1007 Lausanne, Switzerland
88. Library, Culham Laboratory, UKAEA, Abingdon, Oxfordshire, OX14 3DB, England
89. Library, JET Joint Undertaking, Abingdon, Oxfordshire, OX14 3EA, England
90. Library, FOM Instituut voor Plasma-Fysica, Rijnhuizen, Edisonbaan 14, 3439 MN Nieuwegein, Jutphaas, Netherlands
91. Library, Institute of Physics, Academia Sinica, Beijing, Peoples Republic of China
92. Library, International Centre for Theoretical Physics, P.O. Box 586, I-34100 Trieste, Italy
93. Library, Centro Richerche Energia Frascati, C.P. 65, I-00044 Frascati (Roma), Italy

94. Library, Plasma Research Laboratory, Australian National Laboratory, P.O. Box 4, Canberra, ACT 2601, Australia
95. Thermonuclear Library, Japan Atomic Energy Research Institute, Tokai Research Establishment, Tokai, Naka-gun, Ibaraki-ken 311-02, Japan
96. Library, Plasma Physics Laboratory, Kyoto University, Gokasho Uji, Kyoto, Japan
97. Library, Institute for Plasma Physics, Nagoya University, Chikusa-ku, Nagoya 464, Japan
98. Laboratory for Plasma and Fusion Studies, Department of Nuclear Engineering, Seoul National University, Shinrim-dong, Gwanak-ku, Seoul 151, Korea.
99. Office of the Assistant Manager for Energy Research and Development, Department of Energy, Oak Ridge Operations, Oak Ridge, TN 37830
100. M. Roberts, International Programs, Office of Fusion Energy, Office of Energy Research, Germantown ER-52, U.S. Department of Energy, Washington, DC 20545
101. R. E. Price, Office of Fusion Energy, Office of Energy Research, Germantown ER-55, U.S. Department of Energy, Washington, DC 20545
102. V. Chuyanov, I. V. Kurchatov Institute of Atomic Energy, 46 Ulitsa Kurchatova, P.O. Box 3402, Moscow 123182, U.S.S.R.
103. V. A. Glukhikh, Scientific-Research Institute of Electro-Physical Apparatus, 18861 Leningrad, U.S.S.R.
104. H. Iida, Naka Fusion Research Establishment, Japan Atomic Energy Research Inst., Naka-Machi, Naka-Gun, Ibaraki-ken 311-02, Japan
105. B. B. Kadomtsev, I. V. Kurchatov Institute of Atomic Energy, 46 Ulitsa Kurchatova, P.O. Box 3402, Moscow 123182, U.S.S.R.
106. S. M. Kaye, Plasma Physics Laboratory, Princeton University, P.O. Box 451, Princeton, NJ 08543
107. J. Perkins, Lawrence Livermore National Laboratory, P.O. Box 5511, Livermore, CA 94550
108. D. D. Ryutov, Institute of Nuclear Physics, Siberian Branch of the Academy of Sciences of the U.S.S.R., Sovetskaya St. 5, 630090 Novosibirsk, U.S.S.R.
109. W. R. Spears, NET/ITER Team, Max-Planck-Institut, Boltzmannstrasse 2, D-8046 Garching bei Muenchen, Federal Republic of Germany
110. I. Shpigel, Institute of General Physics, U.S.S.R. Academy of Sciences, Ulitsa Vavilova 38, Moscow, U.S.S.R.
111. K. Tomabechi, Naka Fusion Research Establishment, Japan Atomic Energy Research Inst., Naka-Machi, Naka-Gun, Ibaraki-ken 311-02, Japan
112. J. Wesley, General Atomics, P.O. Box 85608, San Diego, CA 92138

113–150. Given Distribution as shown in DOE/OSTI-4500, Energy Research (Distribution Category UC-420, Magnetic Fusion Energy)